(8) Moore, J. W.; Gharapetian, H. M.; Guillet, J. E.; Ito, H.; MacDonald, S. A.; Willson, C. G., in preparation.
(9) Crandall, J. K.; Chang, L.-H. *J. Org. Chem.* **1967**, *32*, 435.
(10) Ito, H.; Miller, D. C.; Willson, C. G. *Macromolecules* **1982**, *15*, 915.
(11) Ito, H.; Willson, C. G.; Frechet, J. M. J.; Farrall, J. M.; Eichler, E. *Macromolecules* **1983**, *16*, 510.
(12) Michaelsen, J. D. U. S. Patent 3 091 532, 1963.
(13) Overberger, C. G.; Schiller, A. M. *J. Polym. Sci., Part C* **1963**, *1*, 325.
(14) Hatada, K.; Kitayama, T.; Okahata, S.; Yuki, H. *Prepr. 43rd Spring Meeting Chem. Soc. Jpn.* **1981**, 1118.
(15) Narita, T.; Imai, N.; Tsuruta, T. *Kogyo Kagaku Zasshi* **1969**, *72*, 994.
(16) Narita, T.; Masaki, A.; Tsuruta, T. *J. Macromol. Sci., Chem.* **1970**, *A4*, 277.
(17) Narita, T.; Yasumura, T.; Tsuruta, T. *Polym. J. (Tokyo)* **1973**, *4*, 421.
(18) Wong, K. H.; Konizer, G.; Smid, J. *J. Am. Chem. Soc.* **1970**, *92*, 666.
(19) Takaki, U.; Hogen-Esch, T. E.; Smid, J. *J. Am. Chem. Soc.* **1971**, *93*, 6760.
(20) Bienvenue, A.; Duchatellier, B. *Tetrahedron* **1972**, *28*, 833.
(21) Naito, I.; Kinoshita, A.; Yonemitsu, T. *Bull. Chem. Soc. Jpn.* **1976**, *49*, 339.
(22) Jackman, L. M.; Wiley, R. H. *J. Chem. Soc.* **1960**, 2881.
(23) Matsuda, M.; Ohshima, K.; Tokura, N. *J. Polym. Sci., Part A* **1964**, *2*, 4271.
(24) Herman, J. J.; Teyssie, Ph. *Macromolecules* **1978**, *11*, 839.
(25) Kawabata, N.; Tsuruta, T.; Furukawa, J. *Makromol. Chem.* **1962**, *51*, 70.
(26) **Note Added in Proof**: After this paper had been submitted for publication, we found an article (Kinoshita, A.; Naito, I. *J. Polym. Sci., Polym. Lett. Ed.* **1983**, *21*, 359) describing radical copolymerizations of alkyl isopropenyl ketones including IPT-BK with styrene.

Molecular Structure and Electronic Property Modification of Poly(diacetylenes)

B. J. Orchard and S. K. Tripathy*

GTE Laboratories Incorporated, Waltham, Massachusetts 02254.
Received December 10, 1985

ABSTRACT: The electronic properties of poly(diacetylenes) were investigated by using the valence effective Hamiltonian (VEH) method. The molecular geometries considered were appropriately optimized. The relative effects of the polymer backbone geometry, the presence of conformational defects along the polymer chain backbone, the chemical/electronic nature of the substituents, and the conformation of the side groups upon the electronic structure were investigated.

I. Introduction

The electronic and optical properties of poly(diacetylenes) have received considerable attention.[1,2] This interest stems from two important considerations: First, poly(diacetylenes) belong to a unique class of macromolecules that can be crystallized to form macroscopic defect-free single crystals[3] with the extended-chain unsaturated backbones stacked parallel to each other. The crystals display a number of different morphologies. The many different side groups that can be part of the monomer structure have a strong influence on the crystalline organization and polymerization behavior in the solid state. Second, the one-dimensional nature of the unsaturated poly(diacetylene) structure implies novel electronic and optical properties. Large and fast (approximately ps) nonlinear optical coefficients have been predicted for these materials. Recent measurements have indeed confirmed these predictions.[4] The materials have the characteristic visible spectrum of a low dimensional semiconductor with an absorption edge in the mid-visible range.

Many fundamental details of these two unique aspects of the poly(diacetylenes) regarding the structural order and the one-dimensional electronic properties have been investigated in detail. Interestingly, however, most investigations dealing with the electronic and optical properties of the diacetylenes treat the lattice of side groups as an appendage whose only primary function is to hold the polymer chain backbones together at a fairly large distance from each other. Thus, most often the diacetylene system, for the electronic property aspects, is modeled as possessing an extended planar trans structure with hydrogen atoms serving as the side groups to satisfy the backbone valence geometry. Hence, most studies to date essentially decouple the electronic states of the side group from those of the backbone. This is not totally inconsistent with the experimental approaches that have been adopted. There are few examples of poly(diacetylene) where side groups have been designed to electronically couple with the backbone states. In one case, Wegner et al.[5] investigated a poly(diacetylene) system with a phenyl group adjacent to the polymer backbone, which would be expected to be more strongly coupled with the backbone, but poor monomer-to-polymer conversion was probably responsible for the lack of subsequent measurements of the electronic and optical properties.

It is clearly seen, however, that side-group organization does strongly influence the electronic properties of the backbone.[6] For example, the thermochromic properties of the poly(diacetylenes) are attributed to the side-group reorganization leading to a change in strain on the backbone. It is in this light that the present investigation was carried out to model the influence on the electronic structure of the backbone of two critical factors; the electronic structure of the side groups and their molecular arrangements vis-a-vis the backbone.

The approach adopted was to use established methodologies that have yielded a reasonable description of the isolated polymer backbone electronic structure in conjuction with molecular mechanics and full geometry optimization to extract the details of the structure property relationships.

In this paper, we report detailed investigations concerning the influence of molecular structure and conformation of the side groups upon the electron-density distribution of the backbone and the resulting electronic properties of the poly(diacetylene) system. Both proposed acetylenic and butatrienic structures were investigated so that the correlation between the chemical/electronic na-

0024-9297/86/2219-1844$01.50/0

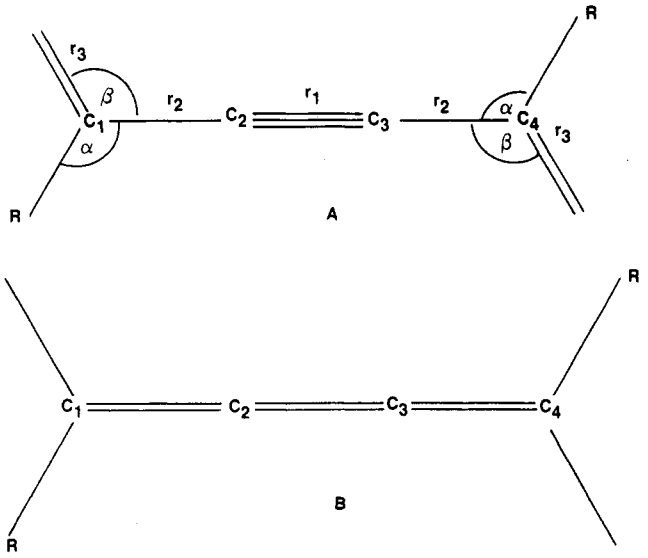

Figure 1. Schematic representation of the valence geometry of the acetylenic (A) and butatrienic (B) structures. The nomenclature is identical with that used by Karpfen.[10]

ture of the side group, the valence geometry of the polymer chain backbone, and the macroscopic electronic properties could be determined. Although the butatrienic form as the ground state has not been established, it is important to determine how dependent the electronic properties are on both the side-group and backbone structures. A combination of approaches has been adopted to arrive at a consistent description of the electronic properties as a function of the discussed parameters. In section II, the utilized methodologies and the influence of the structure and electronic features of the side groups on the electronic properties of the polymer are discussed in detail. Section III summarizes the key issues relating to the polymer chain backbone electronic property modifications via side-group architecture.

II. Results and Discussion

II.1. Molecular Valence Geometry. The precise nature of the molecular valence geometries of the poly(diacetylenes) in the crystalline phase is not well understood, although the acetylenic structure and butatrienic structure (henceforth referred to as structures A and B, respectively, in the tables and figures) are thought to define the extreme limits of possible structures. The acetylenic and butatrienic structures are characterized by relatively localized and highly delocalized electron distributions, respectively. Using ab initio STO-3G,[7] 7s3p/3s,[8] and semiempirical MNDO[9] (modified neglect of diatomic overlap molecular orbital methods), Karpfen[10] analyzed the energetic feasibility of each structure and found the acetylenic backbone to be approximately 12 kcal/mol per repeat lower in energy than the butatrienic form. These two structures are shown in Figure 1, and the geometric parameters for these molecular structures are listed in Table I. Included in Table I, in addition to those supplied by Karpfen,[10] are the MNDO[9] optimized geometries for phenyl-, methyl-, and hydrogen-substituted polymer backbones. (The structures referred to as A and B in Table I are those supplied by Karpfen[10]). In that study,[10] cyclic trimers were used as models of the periodic polymer system. As is seen in Figure 2, this representation is acceptable when the backbone substituents are small atoms, e.g., hydrogen, but the incorporation of more realistic, larger substituents makes this model inadequate as a result of the relative positioning of the substituents. That is, the substituents are in a cis configuration in the cyclic model but are trans in the real system.

To overcome this possible deficiency, long-chain oligomers may be used instead. The total molecular energies were calculated for increasingly larger oligomers by using the MNDO[9] option in the chemical software package Chemlab-II.[11] The corresponding energies per repeat were thus obtained, which reach an asymptotic limit as the size of the oligomer increases. Although the ends of the chains introduce perturbations on intervening chain segments and thus prevent the modeling of a truly periodic polymer system, the use of increasingly larger oligomers rapidly diminishes this deficiency.

The MNDO heats of formation, total molecular energies, and the relative stabilities of tetramers of acetylenic and

Table I
Molecular Valence Geometries of the Acetylenic (A) and Butatrienic (B) Structures[a]

	r_1	r_2	r_3	α	β
A	1.1930	1.4240	1.3210	115.3	123.9
$(C_6H_5)_2$-A	1.2041	1.4159	1.3989	115.3	123.9
$(CH_3)_2$-A	1.2024	1.4180	1.3667	115.3	123.9
H-A′	1.2024	1.4140	1.3579	115.3	123.9
B	1.2480	1.3190	1.4440	119.0	123.7
$(C_6H_5)_2$-B	1.2116	1.4033	1.4384	119.4	123.7
$(CH_3)_2$-B	1.2037	1.4107	1.3865	119.4	123.7
H-B′	1.2041	1.4085	1.3747	119.4	123.7

[a] Bond lengths in angstroms; angles in degrees.

Table II
Relative Heats of Formation per Polymer Repeat As Calculated by MNDO for the Acetylenic (A) and Butatrienic (B) Forms

	ΔH_f[a]	E_{tot}[b]
A	498.6	−106 275.8
B	614.7	−106 159.7
Δ	116.2	116.1
Δ/repeat	14.5	14.5

[a] The reported changes in energy are with respect to structure A and are in units of kcal/mol. [b] In hartrees.

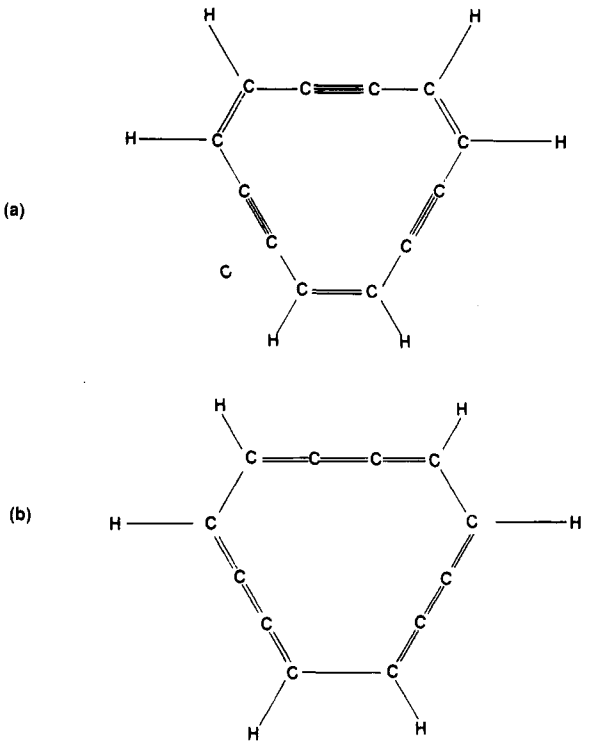

Figure 2. Schematic representation of the cyclic trimer models used by Karpfen.[10]

Table III
MNDO Calculated Atomic Point Charges for an Infinite Polymer for the Acetylenic (A) and Butatrienic (B) Geometries[a]

atom	q_i(A)	q_i(B)	Δ	% Δ
1	0.0332	0.0259	−0.0073	−28.19
2	−0.1040	−0.0980	0.0060	6.12

[a] The changes in point charges are with respect to the acetylenic form.

butatrienic structures are listed in Table II. The results are in good agreement with those found by Karpfen.[10] Karpfen found the acetylenic structure to be more stable than the butatrienic form by 20.0, 12.0, and 11.3 kcal/mol with the STO-3G, 7s3p/3s, and MNDO methods, respectively. These results indicate that relatively short chain segments may be used as models for an infinite periodic polymer chain with negligible loss in accuracy in defining the chain geometries.

II.2. Electron-Density Distribution of the Polymer Backbone. The electronic properties are strongly coupled to the valence geometry of the polymer backbone. For example, the band gap decreases from 2.6 to 0.2 eV going from an acetylenic to a butatriene geometry. To qualitatively determine the effect of changes in the valence geometry on the electron charge distribution, the atomic point charges of the structures were calculated by using the MNDO[9] methodology. Again, as with the molecular energies, to model the periodic nature of the long (infinite) polymer chain, the atomic point charges were calculated as a function of the chain length and the asymptotic limit of the values was taken to be representative of the infinite polymer chain.

As is evident from Table III, a significant decrease of the electron density about atom 1, as depicted in Figure 1, occurs as the degree of delocalization increases. This is the expected result since an increase in delocalization requires the loss of electron density from some nuclear centers. As the backbone transforms from the acetylenic to the butatrienic form, the shift in the electron densities between atoms 1 and 2 flows primarily from atom 1 to atom 2.

II.3. Chemical/Electronic Nature of the Substituents. Clearly, the electronic nature of the substituent has a strong effect on the backbone charge distribution. Methyl and phenyl groups were used as models for electron-donating and electron-withdrawing substituents, respectively. Only one substituent per repeat was used to determine the spatial dependence of the inductive effect along the polymer backbone. The phenyl group was coplanar with the plane of the polymer backbone, which is expected to result in an optimal charge transfer; i.e., delocalization of charge on the backbone is maximized.

The MNDO[9] optimized geometries for the methyl- and phenyl-substituted polymers are listed in Table I. Increasingly longer oligomers were used to calculate the asymptotic values of the geometric parameters. In addition, the optimized valence geometry of the hydrogen-substituted species was calculated by using this approach, in contrast to the cyclic model used previously by Karpfen.[10] The bond angles for all structures were held fixed at the values obtained by Karpfen.[10] As is indicated in Table I, the geometry modification of the backbone upon substitution is small, but is present.

As indicated in Tables IV and V, the phenyl group withdraws electrons from the backbone and results in 121% and 147% decreases in the charge concentration about the connecting backbone atom of the acetylenic and butatrienic structure, respectively. The effect of the substituent rapidly diminishes as the distance from the site of substitution increases.

Table IV
MNDO Calculated Atomic Point Charges for an Infinite Acetylenic Polymer Chain with a Single Hydrogen, Phenyl, or Methyl Group Attached per Repeat[a]

	atom			
	1	2	3	4
A–H	0.0332	−0.1040	−0.1040	0.0332
A–C_6H_5	0.0336	−0.1037	−0.0919	0.0735
A–CH_3	0.0337	−0.1032	−0.0918	−0.0096
$\Delta_{C_6H_5}$	0.0004	0.0003	0.0121	0.0403
% $\Delta_{C_6H_5}$	1.20	2.88	11.63	121.39
Δ_{CH_3}	0.0005	0.0008	0.0122	−0.0428
% Δ_{CH_3}	1.51	.28	11.73	−128.92

[a] The changes in atomic point charges are with respect to the hydrogen-substituted species.

Table V
MNDO Calculated Atomic Point Charges for an Infinite Butatrienic Polymer Chain with a Single Hydrogen, Phenyl, or Methyl Group Attached per Repeat[a]

	atom			
	1	2	3	4
B–H	0.0259	−0.0980	−0.0980	0.0259
B–C_6H_5	0.0163	−0.0907	−0.0843	0.0640
B–CH_3	0.0188	−0.0944	−0.0817	−0.0219
$\Delta_{C_6H_5}$	−0.0096	0.0073	0.0137	0.0381
% $\Delta_{C_6H_5}$	−37.07	7.45	13.98	147.10
Δ_{CH_3}	−0.0071	−0.0036	−0.0163	−0.0478
% Δ_{CH_3}	−27.41	−3.67	16.63	−184.56

[a] The changes in atomic point charges are with respect to the hydrogen-substituted species.

The corresponding results for the methyl-substituted chains are also listed in Tables IV and V. The inductive effect of the methyl group is as strong as the phenyl group for short-range interactions as indicated by the change in charge density at the site of substitution; the changes are almost equal in magnitude but are, naturally, opposite in sign. It appears that the increase in charge concentration at atom 4 is due not only to the methyl substituent but atoms 2 and 3 also donate to atom 4 as indicated by the decrease in density about their centers. The larger changes in the electron density in the delocalized backbone are probably reflective of the greater charge mobility along the chain.

The preceding calculations have established that the electronic nature of the substituent will induce changes in the charge distribution of the polymer backbone. The question now is, do these microscopic changes result in significant alterations of the bulk electronic properties?

The electronic band structure was calculated by using the valence effective Hamiltonian (VEH) method developed by Nicholas and Durand.[12] This method gives results that have ab initio double ζ quality. The bandwidth, bandgap, and Koopman ionization potential of the disubstituted acetylenic and butatrienic structures are listed in Tables VI and VII, respectively.

For the acetylenic structure, both substituents cause a decrease in the bandwidth, although the phenyl group has a considerably stronger effect. The bandgap exhibits similar characteristics. The influence of a phenyl group, coplanar to the backbone, on the backbone electronic structure is dramatic. This will be further discussed in conjunction with the conformational changes in the side group in section II.5. The dramatic shift in the bandgap implies the absorption edge will be significantly red-shifted. This has not been observed for any poly(diacetylene) system but is expected to enhance the third-order non-

Table VI
VEH Calculated Bandwidths (BW), Bandgaps (E(g)), and Ionization Potentials (E(ip)) for the Disubstituted Hydrogen, Phenyl, or Methyl Acetylenic Polymer Structure[a]

	BW	E_g	E_{ip}
A	3.972	2.596	5.338
	312	478	232
	32043	20938	43056
(C_6H_5)-A	1.116	1.769	4.903
	1111	701	253
	8998	14266	39544
$(CH_3)_2$-A	3.265	2.449	5.039
	380	506	246
	26337	19753	40642
$\Delta_{(C_6H_5)_2}$	-2.854	-0.827	-0.435
	799	223	21
	-23045	-6672	-3512
$\Delta_{(CH_3)_2}$	-0.707	-0.147	-0.299
	68	28	14
	-5706	-1185	-2414

[a] The changes in the electronic properties are with respect to the hydrogen-disubstituted polymer. The bandgap and ionization potential are in units of eV, nm, and cm^{-1}.

Table VII
VEH Calculated Bandwidths (BW), Bandgaps (E(g)), and Ionization Potentials (E(ip)) for the Disubstituted Hydrogen, Phenyl, or Methyl Butatrienic Polymer Structure[a]

	BW	E_g	E_{ip}
B	4.816	0.154	4.277
	257	8051	290
	38847	1247	34496
$(C_6H_5)_2$-B	1.878	0.215	4.133
	660	5767	300
	15144	1734	33333
$(CH_3)_2$-B	4.136	0.435	4.032
	300	2850	308
	33360	3512	32521
$\Delta_{(C_6H_5)_2}$	-2.938	0.061	-0.144
	403	-2284	10
	-2370	487	-1163
$\Delta_{(CH_3)_2}$	-0.680	0.281	-0.245
	43	-5201	18
	-5487	2265	-1975

[a] The changes in the electronic properties are with respect to the hydrogen disubstituted polymer. The bandgap and ionization potential are in units of eV, nm, and cm^{-1}.

linear susceptibility by a very large factor. It is an interesting result that both substituents cause changes in the same direction, albeit of different magnitudes. Since the methyl group is not as good an electron donor as the phenyl group is an electron withdrawer, it is possible that a stronger electron donor may exhibit different effects. The butatrienic form, on the other hand, shows different responses to the presence of substituents. Although the change in the bandwidth is similar, the bandgap increases for both substituents with the methyl group having a more pronounced effect.

In summary, the electron distribution along the backbone may be seriously perturbed by the presence of electron-donating or -withdrawing species, which in turn modify the observed macroscopic electronic properties. These results may have a strong bearing for designing poly(diacetylene)-based systems for application in optoelectronics and optics. As subsequent discussions will show, however, the strong electronic interaction of the electroactive side groups to the backbone is sensitive to the side-group conformation. Thus, whether these dramatic effects will be realized, to a great measure, will depend upon the structural aspects of the diacetylene monomer crystals, the topochemical polymerization process and if post-polymerization conformational charges can be brought about via side-group-induced processes.

Table VIII
Polymer Repeat (in Angstroms) as a Function of the Degree of Nonplanarity for Structures A and B

	0°	5°	10°	15°	20°
A	4.896	9.800	9.798	9.796	9.793
B	4.839	9.679	9.678	9.675	9.671

Table IX
VEH Calculated Bandwidths of the Hydrogen-Disubstituted Acetylenic Structure (A) as a Function of Nonplanarity along the Backbone[a]

	0°	5°	10°	15°	20°
eV	3.972	3.538	3.401	3.293	3.129
cm^{-1}	32043	28532	27434	26556	25240
nm	312	350	365	377	396
Δ_{eV}	0.000	-0.434	-0.571	-0.679	-0.843
$\Delta_{cm^{-1}}$	0	-3511	-4609	-5487	-6803
Δ_{nm}	0	38	52	65	84

[a] The changes in the bandwidths are with respect to the planar polymer.

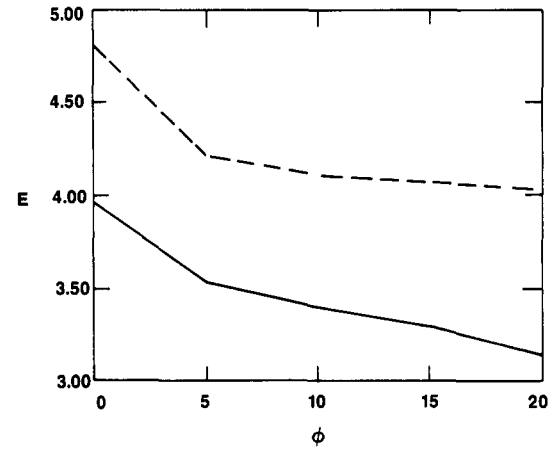

Figure 3. VEH calculated bandwidths (eV) of the acetylenic (solid line) and butatrienic (dashed line) structures as a function of the degree of nonplanarity.

II.4. Conformations of the Polymer Backbone. The electronic properties are not only strongly coupled to the backbone valence geometry and electronic nature of the substituents but are also linked with the conformation of the polymer backbone itself. Within the solid state, the occurrence of nonplanar "defects" should not be strongly prohibited; i.e., rotations of 5–20° about the single bond within the acetylenic model, or smaller rotations about the partial double bond in the butatrienic form, may be possible. This section deals with the effects of periodic nonplanar chain segments on the electronic properties and molecular orbital wave functions. The nonplanar chains were generated by introducing alternating rotations of $+(-)x°$ about the bond formed by atoms 3 and 4. The repeat distances corresponding to these conformations do not differ significantly after the initial shift from nonplanarity and are shown in Table VIII. The unit cell along the chain doubles from symmetry consideration. The electronic properties were calculated with the valence effective Hamiltonian (VEH) method.[12]

The acetylenic and butatrienic chains both undergo sharp decreases in the bandwidth as the chain moves slightly off-planar to +(−)5° as indicated in Tables IX and X and shown in Figure 3. Further increases in the rotation angle ϕ decrease the bandwidth in both cases, but the rate of decrease is less than found for the initial 0–5°-step.

Table X
VEH Calculated Bandwidths of the Hydrogen-Disubstituted Butatrienic Structure (B) as a Function of Nonplanarity along the Backbone[a]

	0°	5°	10°	15°	20°
eV	4.816	4.218	4.109	4.082	4.027
cm^{-1}	38847	34019	33141	32921	32482
nm	257	294	302	304	308
Δ_{eV}	0.000	−0.598	−0.707	−0.734	−0.789
$\Delta_{cm^{-1}}$	0	−4828	−5706	−5926	−6365
Δ_{nm}	0.0	37	45	47	51

[a] The changes in the bandwidths are with respect to the planar polymer.

Table XI
VEH Calculated Bandgaps of the Hydrogen-Disubstituted Acetylenic Structure (A) as a Function of Nonplanarity along the Backbone[a]

	0°	5°	10°	15°	20°
eV	2.596	2.558	2.585	2.612	2.721
cm^{-1}	20938	20631	20850	21070	21947
nm	478	485	480	475	456
Δ_{eV}	0.000	−0.038	−0.011	0.160	0.125
$\Delta_{cm^{-1}}$	0	−307	−88	132	1009
Δ_{nm}	0	7	2	−3	22

[a] The changes in the bandgaps are with respect to the planar polymer.

Table XII
VEH Calculated Bandgaps of the Hydrogen-Disubstituted Butatrienic Structure (B) as a Function of Nonplanarity along the Backbone[a]

	0°	5°	10°	15°	20°
eV	0.154	0.435	0.381	0.299	0.136
cm^{-1}	1247	3512	3073	2414	1097
nm	8021	2848	3255	4142	9113
Δ_{eV}	0.000	0.281	0.227	0.145	−0.018
$\Delta_{cm^{-1}}$	0	2265	1826	1167	−150
Δ_{nm}	0	−5173	−4766	−3879	1092

[a] The changes in the bandgaps are with respect to the planar polymer.

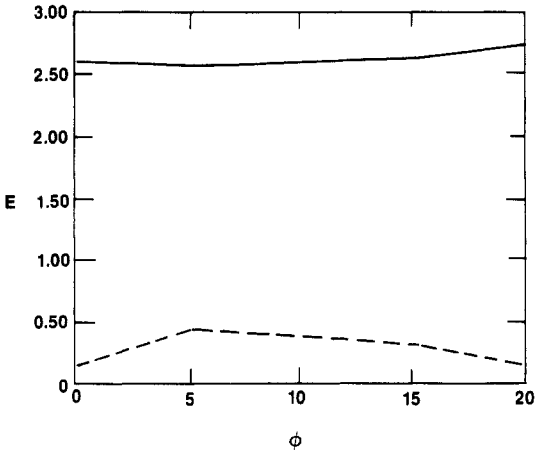

Figure 4.

The bandgaps, which are directly related to the position of the optical transitions, as a function of the bond rotation ϕ are listed in Tables XI and XII and shown in Figure 4. The structures exhibit opposite effects: the bandgap decreases at 5° and then starts to increase with the acetylenic form, but increases and then decreases with the butatrienic structure. Although the changes in the bandgap are fractions of an electronvolt, the corresponding changes in units of wavenumbers (cm^{-1}) are on the order of hundreds and thousands with the acetylenic and the butatrienic structures, respectively. With the butatrienic form, the resulting changes appear to be too large to be correlated with the experimentally observed thermochromic transitions. The planar conformation was arbitrarily chosen as the most probable reference state, although it is possible that a nonplanar conformation may be a more realistic choice. If the conformation with $\phi = +(-)5°$ is the most probable state, then the changes in the bandgap are not as dramatic as the degree of nonplanarity increases.

Table XIII
VEH Calculated Energies (eV) of HOMO and LUMO for the Hydrogen-Disubstituted Acetylenic Structure (A) as a Function of the Degree of Nonplanarity[a]

	0°	5°	10°	15°	20°
E_{HOMO}	−5.34	−5.34	−5.37	−5.37	−5.42
E_{LUMO}	−2.74	−2.78	−2.78	−2.75	−2.70
Δ_{HOMO}	0.00	0.00	−0.03	−0.03	−0.03
% Δ_{HOMO}	0.00	0.00	−0.56	−0.56	−1.50
Δ_{LUMO}	0.00	−0.05	−0.05	−0.01	0.04
% Δ_{LUMO}	0.00	−1.82	−1.82	−0.36	1.46

[a] The changes in energies are with respect to the planar structure.

Table XIV
VEH Calculated Energies (eV) of HOMO and LUMO for the Hydrogen-Disubstituted Butatrienic Structure (B) as a Function of the Degree of Nonplanarity[a]

	0°	5°	10°	15°	20°
E_{LUMO}	−4.28	−4.28	−4.28	−4.20	−4.11
D_{HOMO}	−4.44	−4.65	−4.65	−4.44	−4.20
Δ_{LUMO}	0.00	0.00	0.00	−0.08	−0.17
% Δ_{LUMO}	0.00	0.00	0.00	−1.87	−3.97
Δ_{HOMO}	0.00	0.21	0.21	0.00	−0.24
% Δ_{HOMO}	0.00	4.73	4.73	0.00	−3.41

[a] The changes in energies are with respect to the planar structure.

Table XV
VEH Calculated Ionization Potentials (eV) as a Function of the Nonplanarity of the Acetylenic Polymer Backbone[a]

	0°	5°	10°	15°	20°
eV	5.338	5.338	5.365	5.365	5.420
cm^{-1}	43056	43056	43275	43275	43714
nm	232	232	231	231	229
Δ_{eV}	0.000	0.000	0.027	0.027	0.082
$\Delta_{cm^{-1}}$	0	0	219	219	658
Δ_{nm}	0	0	−1	−1	−3

[a] All changes are with respect to the planar backbone.

As the chain becomes less ordered, the bandgap should increase as a result of the loss of delocalization. The initial decrease in the bandgap of the acetylenic structure is not clearly understood. The decrease found after 5° with butatrienic structure is also disturbing. Although the VEH method was parameterized by using small planar model compounds, it is not expected that such slight deviations from planarity would exceed the limitations of the method.[13] The excited states, i.e., the unoccupied molecular orbitals, on the other hand, are known to have little physical significance within the Hartree–Fock independent electron approximation, and caution must be applied when interpreting the VEH results.[14] The large decrease in the bandgap when only slight rotations, approximately 5°, are introduced results from the decrease in the energy of the lowest unoccupied molecular orbital (LUMO) since the highest occupied (HOMO) remains constant as indicated in Tables XIII and XIV.

The Koopman ionization potentials, which may be related to the dopability of the polymer, are listed in Tables XV and XVI. The acetylenic structure is less sensitive

Table XVI
VEH Calculated Ionization Potentials (eV) as a Function of the Nonplanarity of the Butatrienic Polymer Backbone[a]

	0°	5°	10°	15°	20°
eV	4.277	4.277	4.277	4.195	4.114
cm^{-1}	34496	34496	34496	33838	63179
nm	290	290	290	296	301
Δ_{eV}	0.000	0.000	0.000	−0.082	−0.163
$\Delta_{cm^{-1}}$	0	0	0	−658	−1317
Δ_{nm}	0	0	0	6	11

[a] All changes are with respect to the planar backbone.

Table XVII
VEH Calculated Coefficients of the p(z) Orbitals of HOMO as a Function of the Degree of Nonplanarity for the Acetylenic (A) and Butatrienic (B) Structures

	0°	5°	10°	15°	20°
			Acetylenic		
1	−0.53	−0.37	−0.37	−0.37	−0.37
2	0.45	0.32	0.32	0.31	0.31
3	0.45	0.32	0.32	0.32	0.32
4	−0.52	−0.37	−0.36	−0.36	−0.35
			Butatrienic		
1	0.55	0.39	0.39	0.39	0.38
2	0.46	0.32	0.31	0.31	0.30
3	−0.46	−0.32	−0.32	−0.32	−0.32
4	−0.55	−0.39	−0.38	−0.37	−0.36

Table XVIII
VEH Calculated Coefficients of the p(z) Orbitals of LUMO as a Function of the Degree of Nonplanarity for the Acetylenic (A) and Butatrienic (B) Structures

	0°	5°	10°	15°	20°
			Acetylenic		
1	0.57	0.40	0.40	0.40	0.40
2	0.48	0.34	0.33	0.33	0.33
3	−0.47	−0.33	−0.33	−0.33	−0.34
4	−0.57	−0.40	−0.40	−0.39	−0.38
			Butatrienic		
1	0.54	0.39	0.39	0.38	0.38
2	−0.48	−0.33	−0.33	−0.32	−0.31
3	−0.48	−0.33	−0.33	−0.33	−0.33
4	0.54	0.39	0.38	0.37	0.36

to disorder than the butatrienic form and exhibits opposite characteristics. That is, the ionization potential increases as ϕ increases with the former but decreases for the latter.

The coefficients of the p(z) atomic orbitals (the z axis is perpendicular to the molecular plane while the x axis is coincident with the helical axis) of HOMO and LUMO are listed in Tables XVII and XVIII, respectively. Although the symmetry of the molecular orbitals does not change as ϕ increases, the p(z) coefficients decrease markedly at 5° but essentially remain constant for further increases in ϕ. Thus, the sharp change in the bandwidth as the chain becomes slightly nonplanar is reflected in the shifts in the nature of the p(z) orbitals.

II.5. Substituent Conformation. Many poly(diacetylenes) have substituents that are partially composed of saturated alkyl linkages, e.g., TCDU, PUDD, ETCD, and others.[15] The most probable conformation of the alkyl linkage is an all-trans planar zigzag. The barrier to other low-energy conformations is not substantial, approximately 2–3 kcal/mol. It is conceivable that heat treatment of the polymer sample may induce conformational changes within the substituent that do not necessarily lead to the large reorientations of the substituent. For example, slight rotations about the carbon–carbon bonds in the TCDU substituents do not necessarily lead to the breaking of the stabilizing hydrogen bonds between the side groups. In addition to conformational changes, bending of the bond angle, which connects the alkyl linkage to the backbone, also can occur as demonstrated by the distorted bond angles in TCDU.[16]

Table XIX
VEH Calculated Bandwidths (BW), Bandgaps, and Ionization Potentials for the Substituted Acetylenic Structures for the Various Side-Group Structures[a]

structure	BW	E_g	E_{ip}
1	3.2790	2.3592	5.0009
	378	526	248
	26447	19028	40334
2	3.2572	2.3620	5.0063
	381	525	248
	26271	19050	40378
3	3.2409	2.3592	5.0063
	383	526	248
	26139	19028	40378
4	3.2246	2.3620	5.0063
	384	525	248
	26008	19050	40378
Δ_{21}	−0.0218	0.0028	0.0054
	3	−1	0
	−176	22	44
Δ_{31}	−0.0381	0.0000	0.0054
	5	0	0
	−308	0.0000	44
Δ_{41}	−0.054	0.0028	0.0054
	6	−1	0
	−439	22	44

[a] The units are eV, nm, and cm^{-1}.

The relative sensitivity of the band structure to conformational and geometric changes within the side group was examined. A diethyl-substituted planar acetylenic chain was used as the model. The conformational states of the substituents examined are (1) the trans conformer where the side-group carbon atoms are in the same plane as the polymer backbone; (2) a slightly off-trans conformer that has the terminal carbon atoms rotated 30° out of the plane; (3) a structure that is the same as found in 1, but the ∠CCC bond angles of the substituent are 121°[16] instead of 109.5°; and (4) a conformer that is the same as found in 3 except the terminal alkyl atoms are rotated 30° out of the plane.

The results for the preceeding structures are shown in Table XIX. It appears that the bandwidth is much more sensitive than the bandgap to side-group conformation. Slight perturbations in the side-group conformation cause a 22-cm^{-1} change in the bandgap. An increase in the alkyl bond angle also has a larger effect on the bandwidth. It is possible that the decrease in the through-space interaction between the alkyl σ electrons and the backbone π electrons results in the calculated decrease in the bandwidth. When the bond angle is at 109.5°, the σ and π electrons are in close proximity, which contrasts with the situation found when the bond angle is 121°. Also, as the alkyl bond angle is increased, the bandgap is less sensitive to conformational changes in the substituent, but the bandwidth is more sensitive. This further implies that appropriate conformational transitions in the side group may lead to corresponding transitions in the optical and electronic properties of the backbone.

In addition, calculations were carried out to determine the conformational dependence for phenyl side groups. Initially, the phenyl rings are coplanar with the backbone, and, as reported earlier, the bandgap is 1.12 eV, while the bandwidth is 1.77 eV. As the phenyl rings rotate to 90° out of the plane, the bandgap increases to 2.07 eV and the bandwidth increases to 2.01 eV. Thus, when the substituent is significantly electronically coupled to the polymer backbone, changes in the conformation of the side group

can more strongly influence the macroscopic electronic properties.

III. Conclusion

The purpose of this study was to identify the major structural features that control the macroscopic electronic properties in a poly(diacetylene) system. Clearly, appropriate designing of the side-group architecture including their electronic structure and molecular arrangement can have significant influence on the electronic and optical properties of the poly(diacetylene) assembly. Unfortunately, while the broad considerations for polymerization in a diacetylene monomer single crystal are understood, it is not a priori possible to determine if a monomer system will lead to complete polymerization with the side groups in the desired conformation.

From the calculated changes in the electronic properties relative to the reference planar conformation, the relative significance of the factors can be determined. The coupling strength between the electronic properties and the factors are listed in decreasing order of importance: (1) the molecular valence geometry, (2) the presence of nonplanar segments, (3) the electronic nature of the substituent, and (4) the conformation of the substituent.

Since the electronic activity of the polymer takes place along the backbone, it is to be expected that the molecular valence geometry of the backbone is most strongly coupled with the electronic structure. As a result, any experimental condition that can alter the valence geometry will provide a coarse tuner of the macroscopic electronic properties; it is a coarse tuner in the sense that very slight modifications of the backbone geometry bring about large changes in the electronic band structure. Since the sizes of the atomic displacements necessary within the backbone to induce electronic modifications are small, the valence geometry would not be expected to be strongly coupled with the other structural features discussed. The only possible exception concerns the abundance of nonplanar defects along the backbone as a function of the backbone valence geometry. As the structure becomes more butatrienic, the ease of rotation about the backbone would be diminished since the single bonds contained within the acetylenic model assume some partial double-bond character. Structural factors 3 and 4, on the other hand, would not be as strongly coupled with variations in the backbone valence geometry.

The occurrence of nonplanar defects along the polymer backbone is the second most significant control on the electronic structure. Any structural feature that directly affects the molecular orbital configuration along the backbone will provide a strong lever on the macroscopic electronic properties. As stated earlier, the relative ease of forming a nonplanar defect is largely determined by the structural characteristics of the polymer backbone. In addition, the structural aspects of the side groups will also play a major role in the ability of the backbone to assume nonplanar conformations. For example, Rubner[17] has shown that very large strains can be introduced in certain cross-polymerized diacetylene macromonomer systems which may strongly influence the backbone conformation and introduce other structural defects.

The electronic characteristics of the side group provide a fine tuner of the electronic structure of the polymer. Remarkable changes in the band structure may be brought about by altering the electron-donating or electron-withdrawing ability of the side group. The sensitivity of this tuner can be governed by the coupling strength between the side group and the polymer backbone.

The conformation of the side group is not a strong factor directly, but the indirect effects of conformational variations may be very significant. It is the side groups that largely determine the conformational and crystal-packing properties of the polymer. Thus, any factor that can alter the side-group conformation would unleash any constraint they would have on the more significant structural features, e.g., the molecular valence geometry and the planarity of the backbone.

Acknowledgment. All calculations were carried out on a VAX 11/780 using the chemical modeling package CHEMLAB-II.[11] The VEH program was generously supplied by Dr. J. L. Brēdas. Careful reading of the manuscript by Drs. Sumitendra Mazumdar, Daniel J. Sandman, and Michael Rubner is gratefully acknowledged.

References and Notes

(1) Agrawal, G. P.; Cojan, C.; Flytzanis, C. *Phys. Rev. B: Solid State* **1978**, *17*, 776.
(2) Lieser, G.; Tieke, B.; Wegner, G. *Thin Solid Films* **1980**, *68*, 77.
(3) Thakur, M.; Meyler, S. *Macromolecules* **1985**, *18*, 2342.
(4) (a) Carter, G. M.; Chen, Y. J.; Tripathy, S. K. *Appl. Phys. Lett.* **1983**, *43*, 891. (b) Carter, G. M.; Thakur, M. K.; Chen, J. Y.; Hryniewicz, J. *Appl. Phys. Lett.* **1985**, *47*, 457.
(5) Wegner, G. *Polym. Lett.* **1971**, *9*, 133.
(6) Chance, R. R.; Baughman, R. H.; Muller, H.; Eckhardt, C. J. *J. Chem. Phys.* **1977**, *67*, 3616.
(7) Hehre, W. J.; Stewart, R. F.; Pople, J. A. *J. Chem. Phys.* **1969**, *51*, 2657.
(8) Huzinaga, S. *J. Chem. Phys.* **1965**, *42*, 1293.
(9) Dewar, M. J. S.; Thiel, W. *J. Am. Chem. Soc.* **1977**, *99*, 4899.
(10) Karpfen, A. *J. Phys. C.*: **1980**, *13*, 5673.
(11) Pearlstein, R. A. *Chemlab-II Reference Manual*; Molecular Design: San Leandro, CA, 1985.
(12) Nicholas, G.; Durand, Ph. *J. Chem. Phys.* **1979**, *70*, 2020; **1980**, *72*, 453.
(13) Private communication with J. L. Brēdas.
(14) Brēdas, J. L.; Chance, R. R.; Baughman, R. H.; Silbey, R. *J. Chem. Phys.* **1982**, *76*, 3673.
(15) "Polydiacetylenes" in *Advances in Polymer Science*; Cantow, H. J., Ed.; Springer-Verlag: Berlin, 1984.
(16) Enkelmann, V.; Lando, J. B. *Acta Crystallogr.* **1976**, *B34*, 2352.
(17) Rubner, M., submitted for publication.